ARTICLE
JOURNAL OF UNIVERSITY OF BABYLON
For ENGINEERING SCIENCES (JUBES)
Vol.31, No.5.| 2023

Nonlinear Analysis of Slurry Infiltrated Fiber Concrete Vierendeel Truss

Raghda A. Naser[1] **Khalid K. Shadhan**[2]

[1,2]*Civil Engineering Department, University of Babylon, Hilla, Iraq.*

raghda.nasser.engh369@student.uobabylon.edu.iq

Received:	4/6/2023	Accepted:	25/6/2023	Published:	10/8/2023

Abstract

The behavior of slurry-infiltrated fiber concrete (SIFCON) Vierendeel trusses under the applied load by employing numerical analyses for the studied trusses is the aim of this paper. The nonlinear behavior of such trusses have been investigated using the finite element software ABAQUS. A finite element model of three dimensions has been used. The structural behaviour is presented in terms of ultimate load, crack pattern and deflection. The numerical results show that the simulated numerical behavior has a good agreement with the experimental results of the pervious tested specimens and the failure mode similar to that recorded in the experimental test. It was found that when the openings are present, the usual flow of stresses is disrupted or interrupted, which causes stress concentration and early cracking in the area of the opening.

Keywords: SIFCON, ABAQUS, Vierendeel Truss, ultimate load, crack pattern.

Introduction

A number of rectangular or trapezoidal panels missing the diagonal elements making up a Vierendeel (girder) truss. Instead of the typical triangular voids used in pin joints, these trusses use rectangular openings with rigid connections between the parts.
Vierendeel truss is easier to shape and place, has simple details due to the small number of members at a joint, and can be pre-cast or cast in place. It also has aesthetic qualities. The various types of Vierendeel trusses used in practice are displayed in Figure 1 [1].

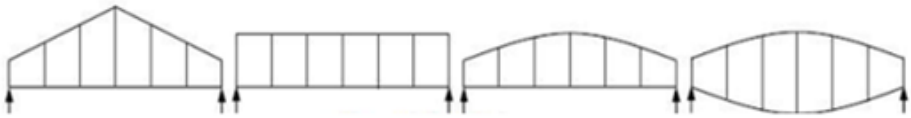

Figure 1: Types of Vierendeel trusses

Pararmasiveam(1980)[2], studied the analysis of Vierendeel frames under anti symmetrical loading by reducing them to that of open frames. The slope-shear equation concept was

ISSN: 2616 - 9916
www.journalofbabylon.com | Journal.eng@uobabylon.edu.iq | info@journalofbabylon.com

ISSN: 2616 - 9916
www.journalofbabylon.com | Journal.eng@uobabylon.edu.iq | info@journalofbabylon.com

presented. This concept resulting in a simpler solution, because the shear force in the chord parts is statically determinant, which is an important property. Since the sum of external loads above a column's section determines its shear at any given point. In this situation, it is more practical to formulate slope-shear equations, which express the member's end moment in terms of the member's end slope and shear. Since the deflection is not known these approaches are preferred to the slope deflection equation.

Alwash (1995)[3], proposed a general nonlinear stiffness method for the analysis of reinforced concrete frames. Then, this manner was utilized for the analysis of reinforced concrete Vierendeel trusses, where different parameters were included. These parameters combined the effects of geometric nonlinearity, shear, material nonlinearity moment-axial force interaction, unloading and element end rigidity. Experimentally, three models of reinforced concrete Vierendeel trusses of different shapes and dimensions were casted and tested up to failure. The results were compared with those obtained theoretically by the proposed method. It was found that the proposed methods were efficient for modeling such structures.

Shuber (1996) [4], proposed a method for analysis of parallel chords Vierendeel trusses with rigid ended vertical members. This method included derivation of three general equations representing the relation between the redundant unknown (moment, shear and axial forces) at the center of the panel. The solution of the derived equations was accomplished by using successive approximations (Gauss Sedil). Several Vierendeel trusses were analyzed with varying number of panels, load case and member dimensions to show the accuracy of the proposed method.

Geometry of specimens

The properties of the numerical simulated models are based on the previously tested specimens [5]. The dimensions of all models have 1350 , 250 for length width, respectively.

Table 1: Properties of the Specimens

Group No.	Specimen designation	Void shape	Void ratio $\frac{V.voids}{V.total}$	Thickness mm	Schematic diagram
Control	VS0.4T60	Square	0.4	60	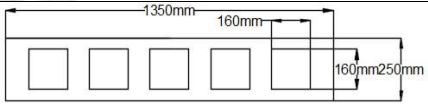
I	VC0.4T60	Circle	0.4	60	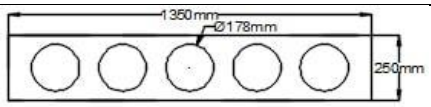
	VT0.4T60	Triangle	0.4	60	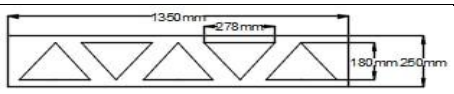

ISSN: 2616 - 9916
www.journalofbabylon.com | Journal.eng@uobabylon.edu.iq | info@journalofbabylon.com

II	VS0.6T60	Square	0.6	60	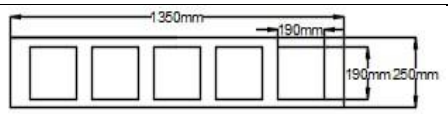
	VS0.2T60	Square	0.2	60	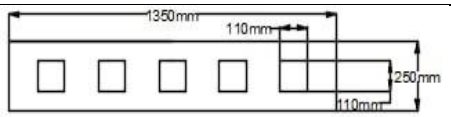
	VS0T60	Without openings	solid	60	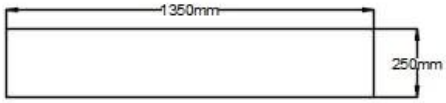
III	VS0.4T40	Square	0.4	40	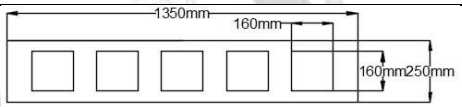
	VS0.4T80	Square	0.4	80	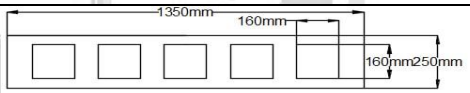

Table 2: SIFCON mechanical properties

f'_c **MPa**	f_t **MPa**	f_r **MPa**
132.38	25.25	38.74

Finite element

It is advised that concrete be represented with an eight-nodded linear 3D brick solid element with reduced integration (C3D8R) in order to simulate the actual behavior of specimens [6] as shown in Figure 2. For a wide range of applications, this element type offers reliable solutions. Eight nodes with three degrees of freedom are present in each 3D solid element. It is applicable to both linear and complex non-linear analyses including contact, plasticity, and big deformations. Similar to Vierendeel truss, The steel plates were modeled using the three-dimensional solid element (C3D8R) in both the loading and supporting positions.

ISSN: 2616 - 9916
www.journalofbabylon.com | Journal.eng@uobabylon.edu.iq | info@journalofbabylon.com

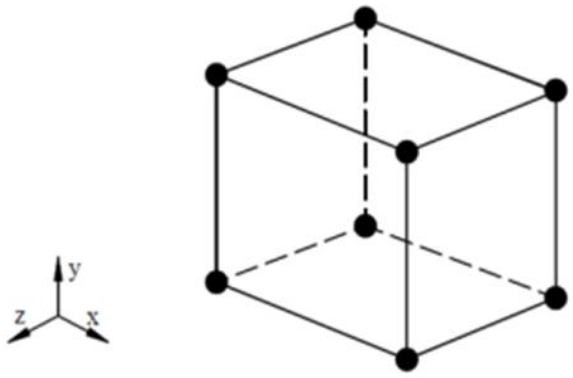

Figure 2: C3D8R element used in in ABAQUS[7].

Concrete Damaged Plasticity in ABAQUS

All structural kinds of reinforced or unreinforced concrete as well as other quasi-brittle materials subjected to monotonic, cyclic, or dynamic loads can be modeled using concrete damaged plasticity. This model is based on a linked damage plasticity theory, and Lubliner et al.'s proposed yield surface drives the multi-axial behavior of concrete in the damaged plasticity model [8]. In this concept, the two basic failure mechanisms for concrete are tensile cracking and compressive crushing. Additionally, this model takes into account material degradation for both tension and compression behavior. By defining the tensile damage parameter (dt) and compressive damage parameter (dc), two scalar parameters for concrete degradation under cyclic and dynamic loadings are taken into consideration.

Uniaxial Behavior of Concrete

Stress Strain Curve of SIFCON in Compression

The following model developed by **(Homrich and Naaman)** [9]was successfully used in obtaining the behavior of SIFCON in direct uniaxial compression.

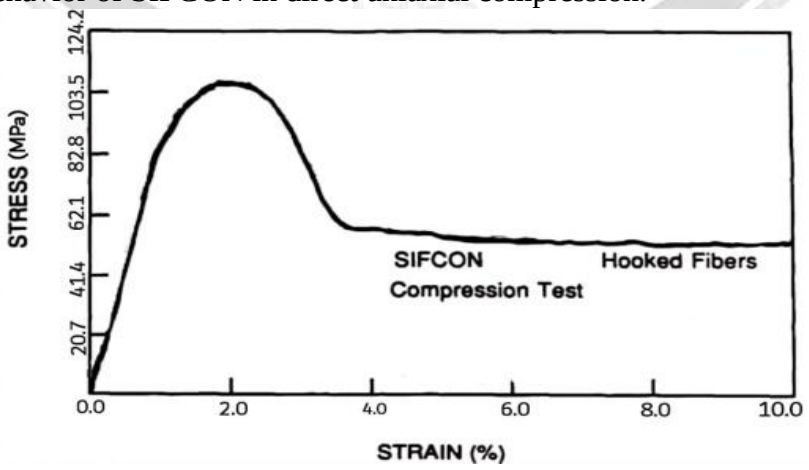

Figure 3: Stress Strain Curve for Compression[9]

ISSN: 2616 - 9916
www.journalofbabylon.com | Journal.eng@uobabylon.edu.iq | info@journalofbabylon.com

- **Ascending Branch**

An equation of the following form was used to simulate the ascending branch of SIFCON's stress-strain compression curve:

$$f = f_\circ \left[1 - \left(1 - \frac{\varepsilon}{\varepsilon_\circ}\right)^A\right] \quad (1)$$

Where:
f - compressive stress (MPa)
$f_\circ$ - maximum compressive stress(MPa)
ε - strain
$\varepsilon_\circ$ - strain at maximum stress

$$A = E\ \varepsilon_\circ / f_\circ \quad (2)$$

E, the initial tangent modulus, is calculable using the law of mixture:

$$E = \gamma_1 V_f E_{fibers} + (1 - V_f) E_{slurry} \quad (3)$$

Where:
V_f - fiber's volume fraction
γ_1- factor often taken to be 1 for compressive loading
E_{fibers}- 206842 MPa
E_{slurry}- 6894 MPa
the strain at peak stress, $\varepsilon_\circ$,can be determined:

$$\varepsilon_\circ = \varepsilon_{initial} + K_1 V_f l/\emptyset \quad (4)$$

Where:
$\varepsilon_{initial}$ - 0.005
K_1- 0.00138
l - fiber length (mm)
$\emptyset$ - fiber diameter (mm)

- **Descending Branch**

An equation of the following form was used to simulate the descending branch of SIFCON's stress-strain compression curve:

$$f = (f_\circ - f_{pl}) \mathrm{Exp}[-b(\varepsilon - \varepsilon_\circ)^m] + f_{pl} \quad (5)$$

$$m = [1 + \ln[\frac{f_i - f_{pl}}{f_\circ - f_{pl}}]^{-1} \quad (6)$$

$$b = [\frac{m-1}{m}](\varepsilon_i - \varepsilon_\circ)^{-m} \quad (7)$$

f_{pl} - post peak plateau stress (MPa)
$f_\circ$ - peak stress (MPa)
f_i - stress at post peak inflection point (MPa)
$\varepsilon_\circ$ - strain at peak stress
ε_i - strain at post peak inflection point
b, m - controlling parameters to be determined

$$f_{pl} = V_f l/\emptyset (K_{31} + K_{32}\sqrt{f_\circ}) \quad (8)$$

K_{31} - 1.38 MPa for hooked fibers
K_{32} - 0.055 MPa for all types of fiber

ISSN: 2616 - 9916
www.journalofbabylon.com | Journal.eng@uobabylon.edu.iq | info@journalofbabylon.com

Stress-Displacement Curve of SIFCON in Tension

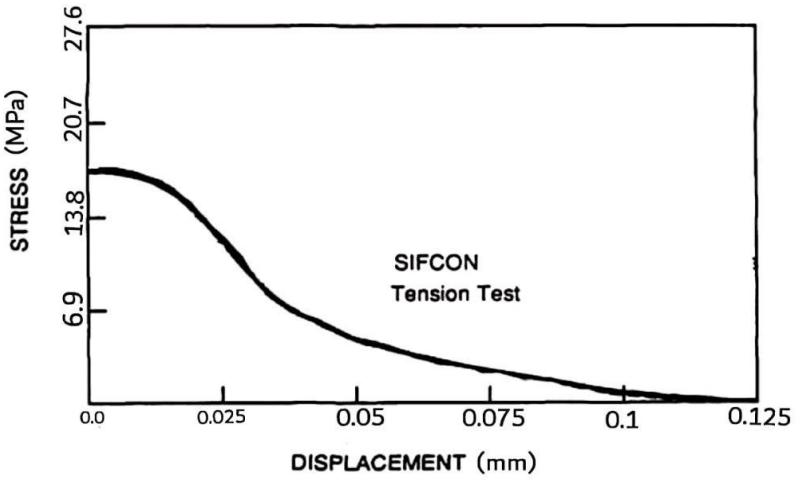

Figure 4: Stress Displacement Curve for Tension [9]

$$f = f_{\circ t}[\mathrm{Exp}(-b(\delta)^m) - c(\delta)] \quad (9)$$

$$c = 2\mathrm{Exp}\left[-b\left(\frac{l}{2}\right)^m\right]/l \quad (10)$$

$$b = \frac{m-1}{[m(\delta_{it})^m]} \quad (11)$$

$$m = \frac{1}{1+\ln\left[\frac{f_{it}}{f_{\circ t}}+c\delta_{it}\right]} \quad (12)$$

Where:
f - tensile stress (MPa)
$f_{\circ t}$- maximum tensile stress= $f_{pl}/3$ (MPa)
f_{it} - tensile stress at inflection point = $0.6f_{\circ t}$(MPa)
δ- tensile crack displacement (mm)
δ_{it}- crack displacement at inflection point =$0.01V_f\, l^2/\emptyset$ (mm)

Concrete Damaged Plasticity Parameters in Triaxial Loading State

A collection of five parameters is needed to fully characterize the plastic behavior of concrete when using the equation for triaxial stress as input to the finite element program ABAQUS;
Ψ, Dilation angle: the failure surface's inclination to the hydrostatic axis as measured in the meridian plane. Physically, the dilation angle is understood as the internal friction angle of the concrete. Its maximum value is equal to 56.3°, while its minimum value is quite near to 0°[10]. By putting geometry through many tries in an effort to achieve suitable failure that is consistent with the recorded experimental failure mechanism, the value of dilation angle was taken as (40^o) for all specimens.
ϵ : The plastic potential eccentricity, which is a small positive number, expresses the rate that the plastic potential hyperbola approaches its asymptote. the ratio of Tensile strength to compressive strength can be used to calculate it. It is recommended to assume ϵ = 0.1 in the CDP model [10].
Fb0/fc0: is the ratio of the initial uniaxial and equiaxial compressive yield stresses [10]. In ABAQUS, the default value is 1.16.

ISSN: 2616 - 9916
www.journalofbabylon.com | Journal.eng@uobabylon.edu.iq | info@journalofbabylon.com

K: is, for any specified value of the pressure invariant at initial yield, the ratio of the second stress invariant in the tensile meridian to the compressive meridian. It is (0.5< Kc≤1)and is used to describe the multi-axial behavior of concrete.[10]. In ABAQUS, the default value is (0.667).

μ: is the parameter for viscosity. The ABAQUS/Explicit analysis is unaffected, although it does help an ABAQUS/Standard analysis converge. According to (Malm)[11] μ=10-7 is advised because the characteristic time increment should be small.

Steel Plate Model Properties

The equation below, with solid elements for all models, was used to represent the steel plates using an isotropic linear elastic material. The loading and supporting plate material is chosen with the premise that big deformations or stress singularities in the plates won't cause problems

$$fs = E_s\varepsilon_s\ (MPa),\ \ \varepsilon s \leq \varepsilon \qquad (13)$$

Model Geometry and Boundary Conditions

To provide a precise approximation of the general behavior and failure mode for SIFCON Vierendeel specimens, 3D simulations were carried out. By considering symmetry of the specimens, only one quarter of the specimens were used for the simulations. Figure 5 provides a 3D view of the FE model's geometry that was created for the control truss. The truss's X-axis runs parallel to its longitudinal axis, and its cross section is represented in the Y-Z plane.

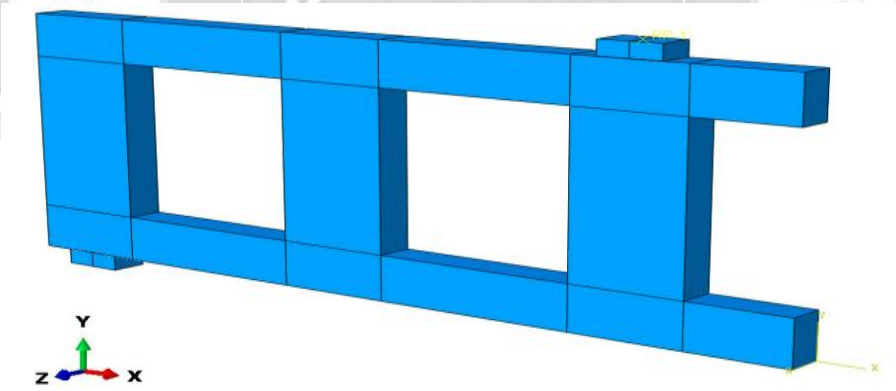

Figure 5: 3D view of the Vierendeel truss F.E. model

The "mechanical fraction" option is used for connecting steel plates to the specimen in both the loading and supporting positions, with a frictional coefficient of 0.3[12].

The specimen is only simply supported, thus it features a hinge in one of its ends that restricts translations in the x- and y-directions. Additionally, simple support restraint translation in the y-directions is imposed at the other end. On a line drawn across the center of the steel plates, the real constraints are inserted along the specimen's width.

Two symmetry planes are taken into consideration because commercial FE software can be highly time-intensive. The first one is placed in the center of the specimen along its width. An x-axis constraint is taken into consideration for this symmetry plane. In addition, a second

ISSN: 2616 - 9916
www.journalofbabylon.com | Journal.eng@uobabylon.edu.iq | info@journalofbabylon.com

plane is taken into account along the length, and in this plane, the translation along the z-axis is restricted.

Figure 6 gives details regarding the typical boundary conditions of the specimens used for the simulations.

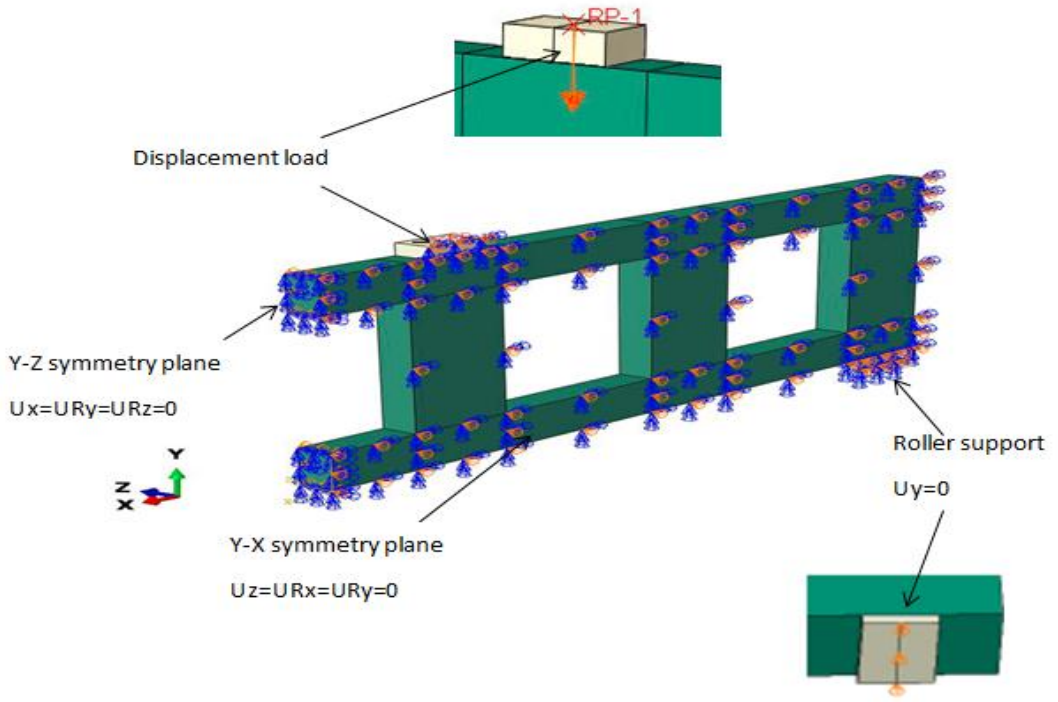

Figure 6: Typical applied load and boundary conditions of modeled trusses

The small size element increases the accuracy of the results of the finite element, therefore, the mesh size was taken 5mm, which give a reasonable result at the accepted time of analysis.

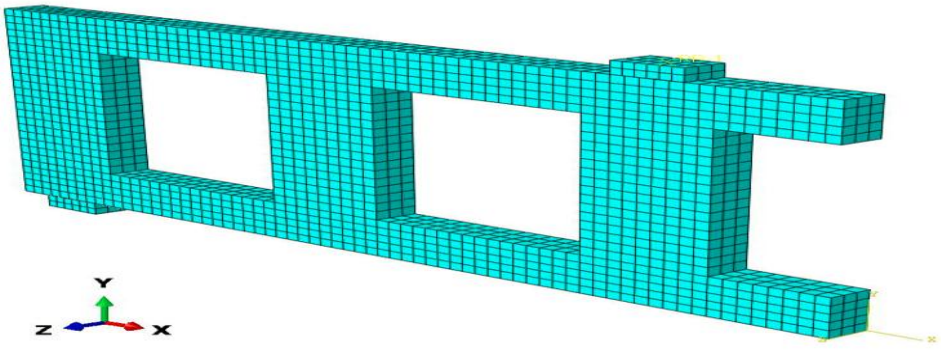

Figure 7: Typical mesh applied for the specimens

ISSN: 2616 - 9916
www.journalofbabylon.com | Journal.eng@uobabylon.edu.iq | info@journalofbabylon.com

Results and Discussion

For all tested specimens, the finite element analysis results produced by the ABAQUS program have been compared with the pervious results of the experimental [5].

Table 3: Experimental and Numerical Results for all specimens

Specimens	Ultimate load (KN)		$\frac{p_{u)Num}-p_{u)EXP}}{p_{u)EXP}}$ %	Max. Deflection(mm)		$\frac{\Delta_{u)Num}-\Delta_{u)EXP}}{\Delta_{u)EXP}}$ %
	$p_{u)EXP}$	$p_{u)Num}$		$\Delta_{u)EXP}$	$\Delta_{u)Num}$	
VS0.4T60	38	38	0	6.74	6.82	1.2
VC0.4T60	42	41	-2	5.57	4.4	-21
VT0.4T60	34	36	5.88	4.51	3.52	-21.9
VS0.6T60	15	15	0	10.82	7.81	-27.8
VS0.2T60	53	54	1.89	4.65	3.57	-23.2
VS0T60	95	101	6.32	5.57	6.4	14.9
VS0.4T40	20	22	10	6.62	6.81	2.8
VS0.4T80	49	52	6.12	7.93	7.15	-9.8
Average			+3.5%			-10.6%

Load - Deflection Response

The relationship between load and deflection represents the behavior of the investigated members along the period of the loading history. The FEM's prediction of the load-mid span deflection was in good agreement with the experimental data. But compared to the similar responses from the experiments, it showed stiffer responses. There may be a variety of causes for greater stiffness in FEM. In the case of the experiments, the primary cause is the

development of microcracks gained on by dry shrinkage, the handling of concrete, environmental factors, and so on. Such micro cracks are not simulated by FEM[13].

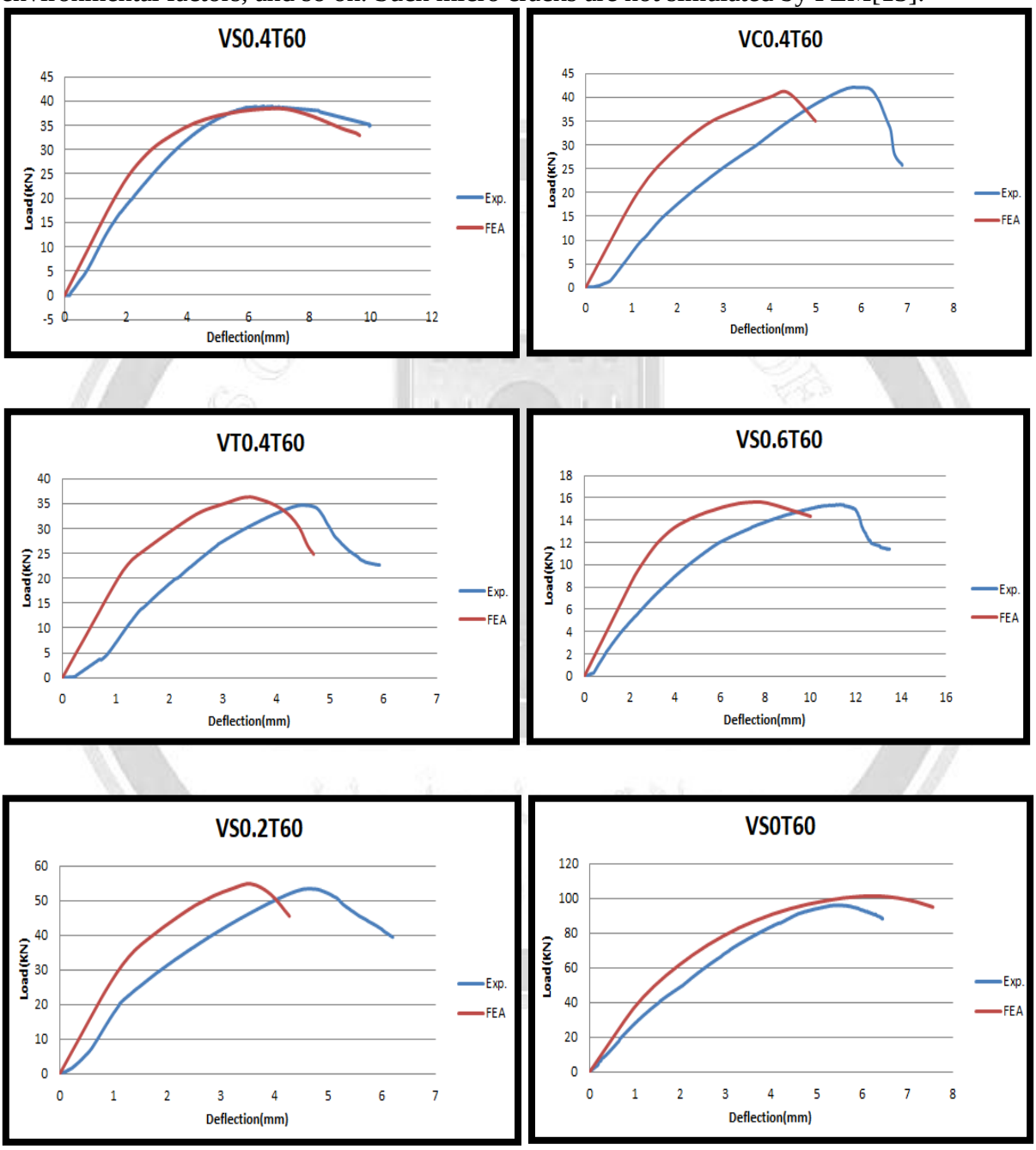

ISSN: 2616 - 9916
www.journalofbabylon.com | Journal.eng@uobabylon.edu.iq | info@journalofbabylon.com

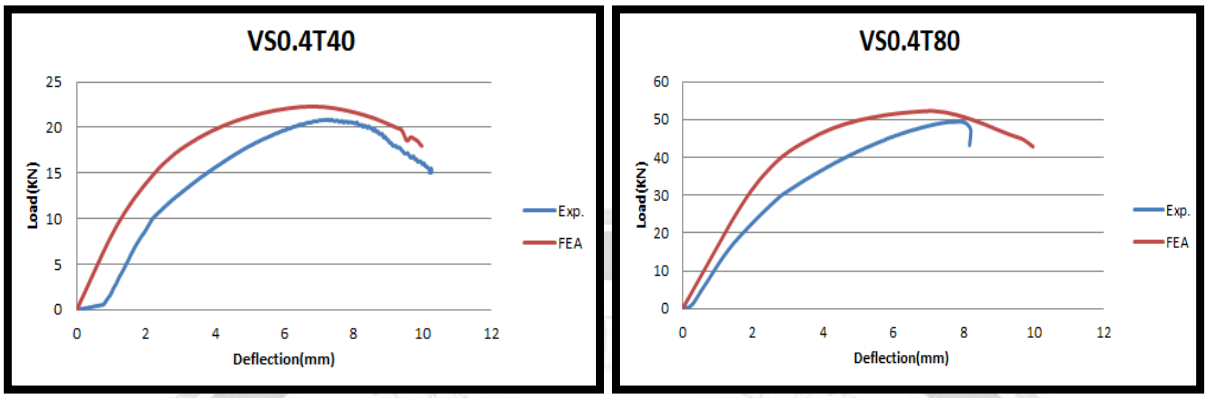

Figure 8: Experimental and numerical load-mid span deflection curves for specimens

Deflection

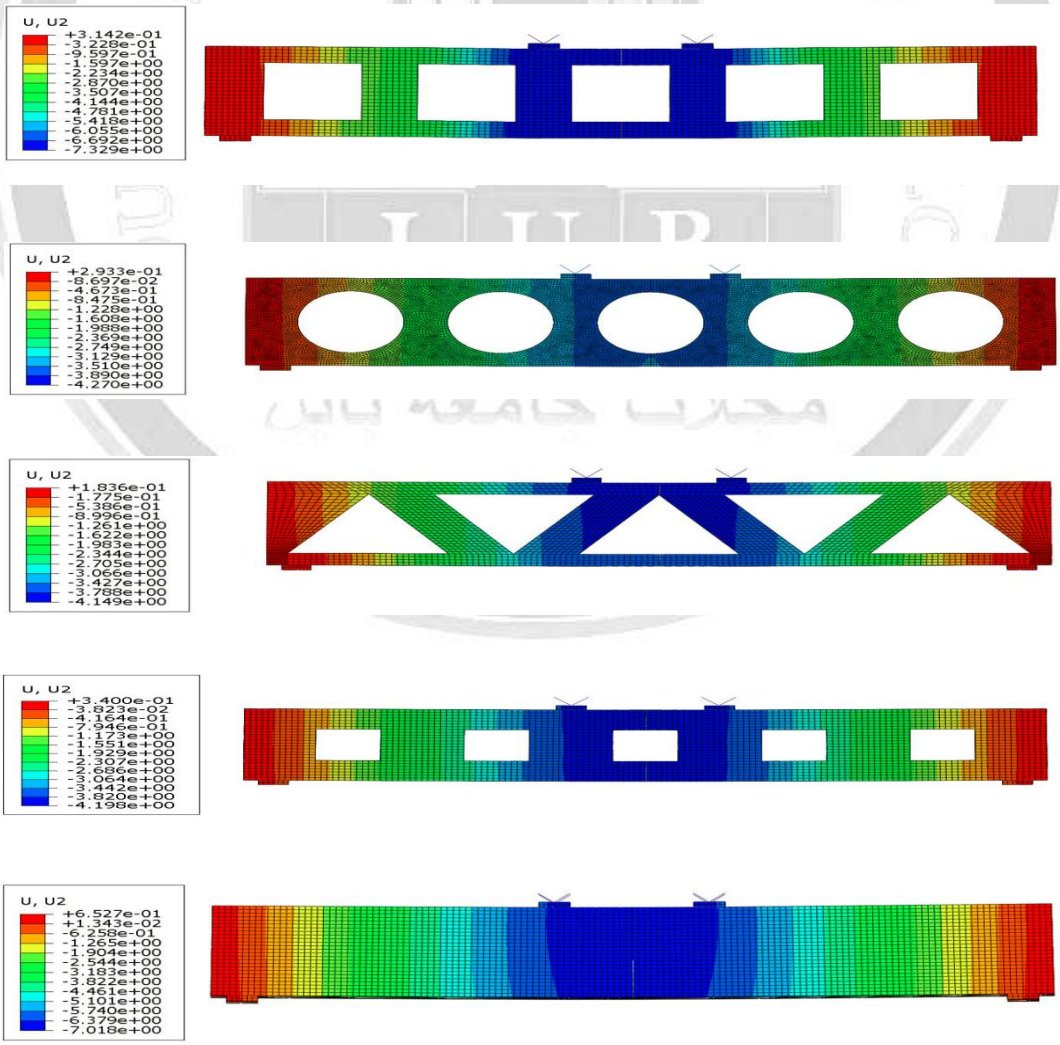

ISSN: 2616 - 9916
www.journalofbabylon.com | Journal.eng@uobabylon.edu.iq | info@journalofbabylon.com

ISSN: 2616 - 9916
www.journalofbabylon.com | Journal.eng@uobabylon.edu.iq | info@journalofbabylon.com

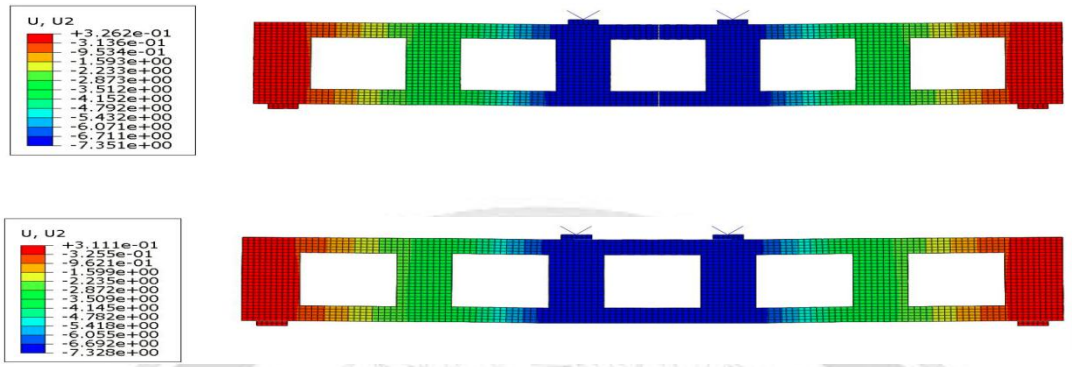

Figure 9: Profile of deflected shape from ABAQUS program for specimens (VS0.4T60, VC0.4T60, VT0.4T60, VS0.6T60, VS0.2T60, VS0T60, VS0.4T40, VS0.4T80) respectively.

Stress Behavior at Ultimate Load

Figure 10 shows the stress (σ max principal) distribution at ultimate load for the specimens. As shown in Figure, a portion from the compression area was cut off by the presence of the openings and leading to stresses concentrated at its sides. This is the main reason for the reduction in the ultimate load compared with the solid specimen.

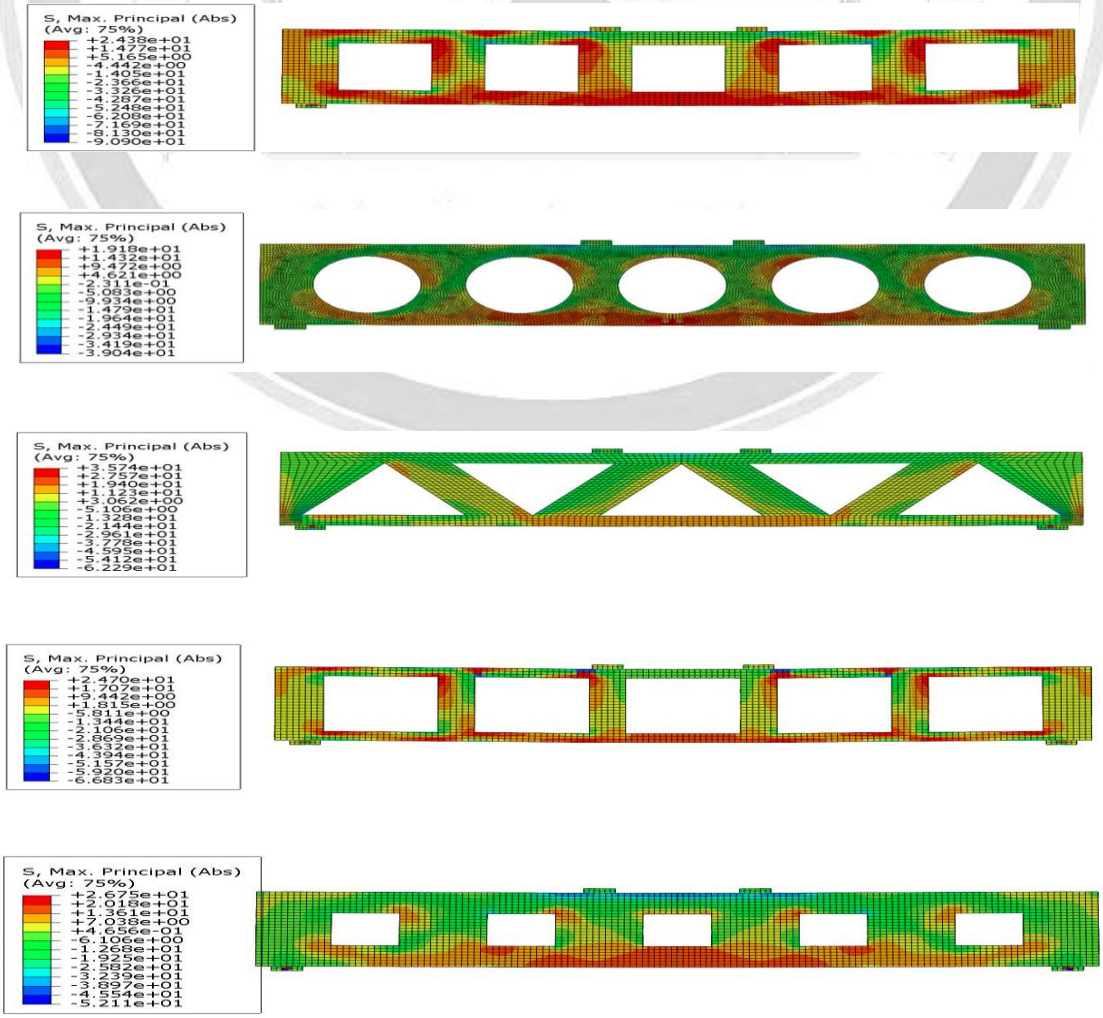

ISSN: 2616 - 9916
www.journalofbabylon.com | Journal.eng@uobabylon.edu.iq | info@journalofbabylon.com

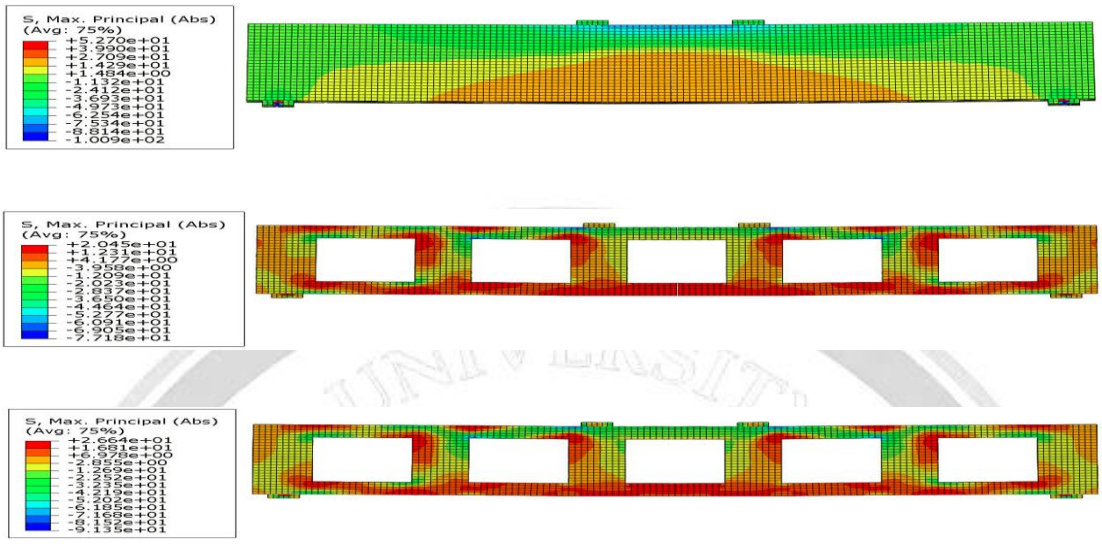

Figure 10: Stresses (σ max principal) distribution of FEM at ultimate load for specimens (VS0.4T60, VC0.4T60, VT0.4T60, VS0.6T60, VS0.2T60, VS0T60, VS0.4T40, VS0.4T80) respectively.

Crack Pattern and Modes of Failure

Crack patterns in concrete at failure stages of the tested specimens which obtained by ABAQUS can show in Figure 11 to Figure 18. By comparing between them, can noticed acceptable match between experimental and theoretical results.

Figure 11: Cracking patterns of FEM versus experimental study for VS0.4T60

ISSN: 2616 - 9916
www.journalofbabylon.com | Journal.eng@uobabylon.edu.iq | info@journalofbabylon.com

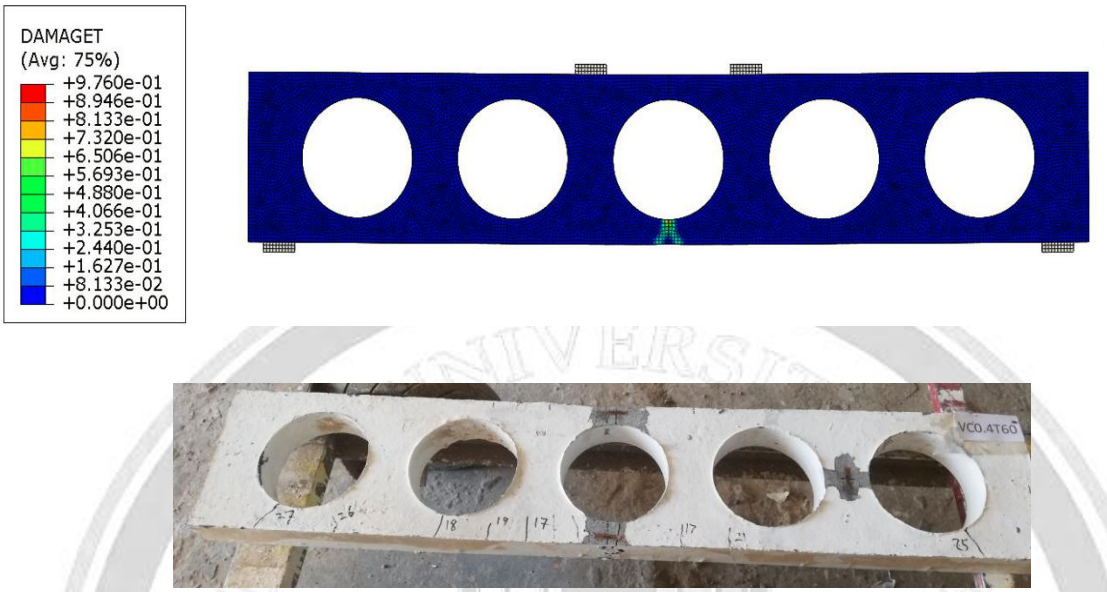

Figure 12: Cracking patterns of FEM versus experimental study for VC0.4T60

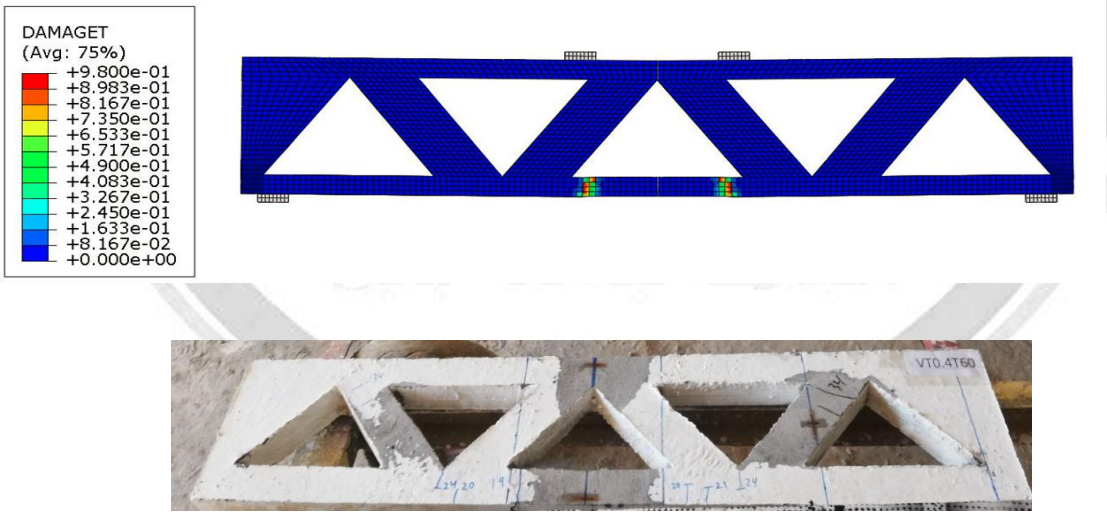

Figure 13: Cracking patterns of FEM versus experimental study for VT0.4T60

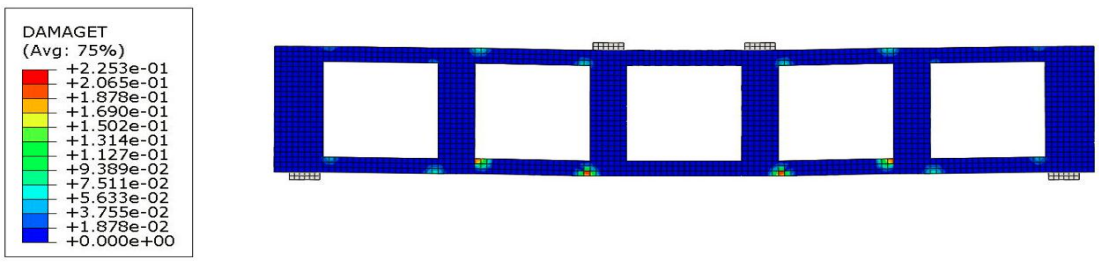

ISSN: 2616 - 9916
www.journalofbabylon.com | Journal.eng@uobabylon.edu.iq | info@journalofbabylon.com

Figure 14: Cracking patterns of FEM versus experimental study for VS0.6T60

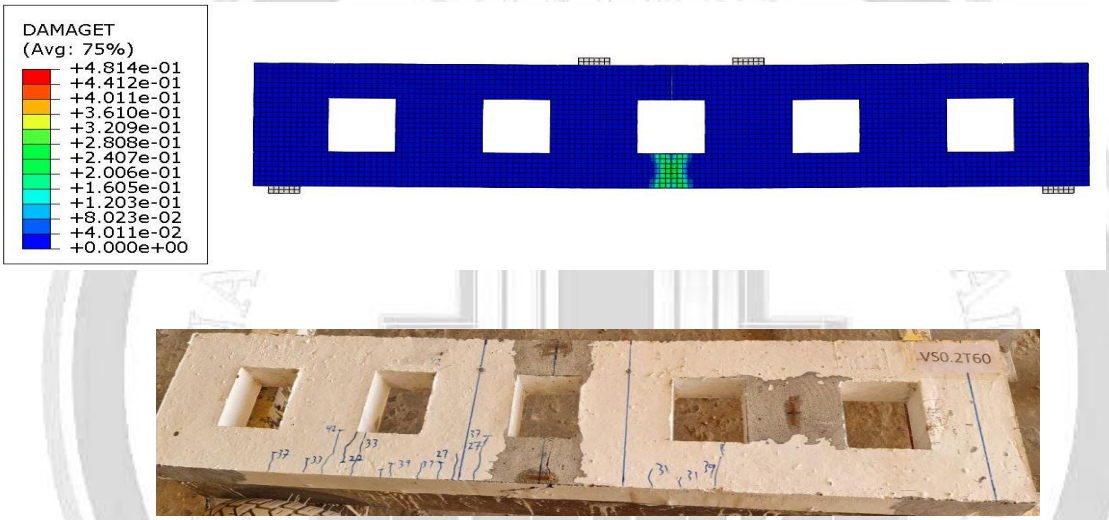

Figure 15: Cracking patterns of FEM versus experimental study for VS0.2T60

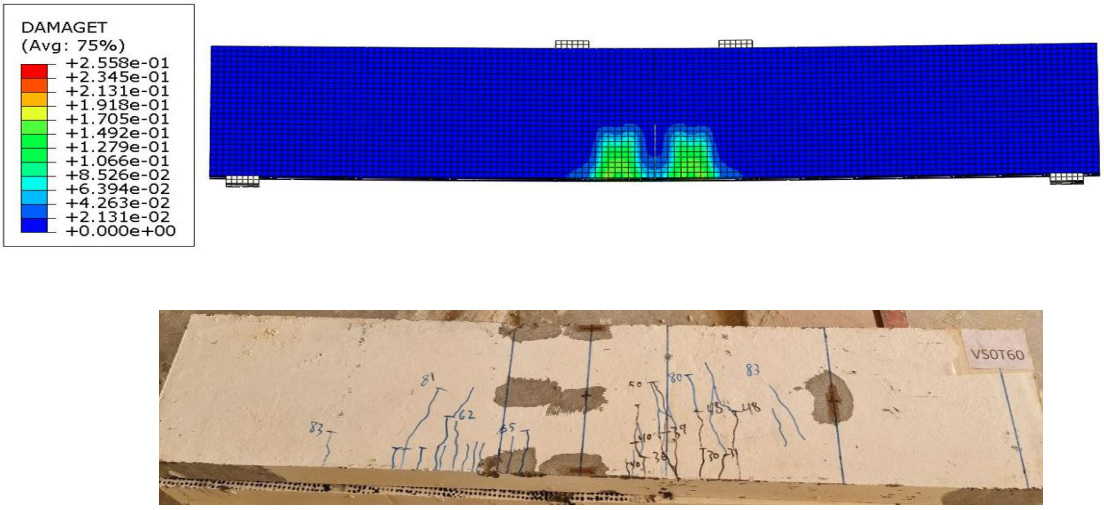

Figure 16:Cracking patterns of FEM versus experimental study for VS0T60

ISSN: 2616 - 9916
www.journalofbabylon.com | Journal.eng@uobabylon.edu.iq | info@journalofbabylon.com

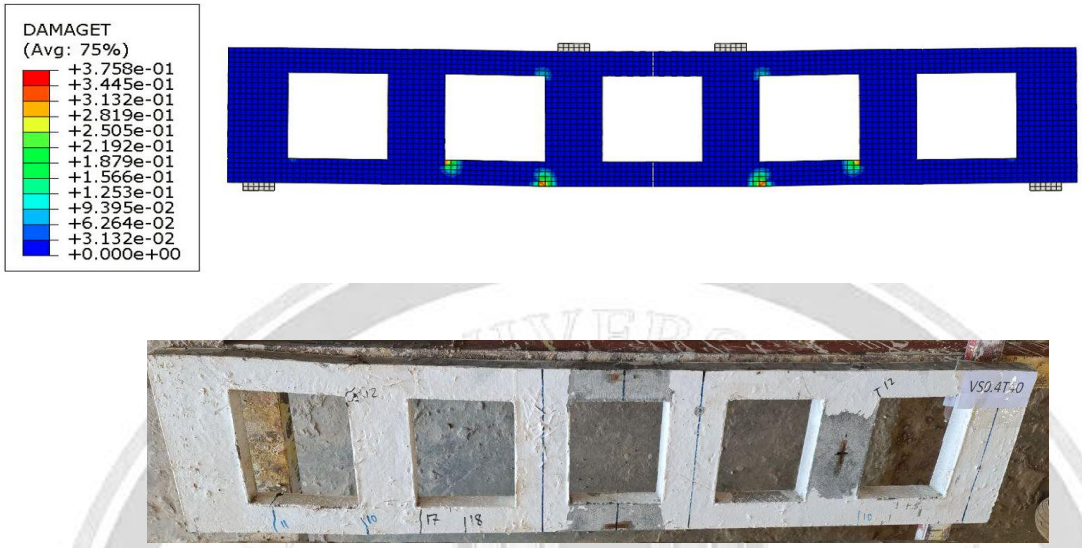

Figure 17:Cracking patterns of FEM versus experimental study for VS0.4T40

Figure 18:Cracking patterns of FEM versus experimental study for VS0.4T80

Conclusions

In this study, numerical analysis for number of Vierendeel specimens was performed and verified with those specimens of experimental tests, which were conducted in a previous study. The analysis results result in the following conclusion to be made:

- The CDP model-based 3D finite element analysis by ABAQUS package is valid for the analysis of SIFCON Vierendeel trusses. The general response of load deflection curves, The FEM predictions for the tested specimens' ultimate load and mid-span deflection were in good agreement with the results of the experiments. The average difference in results was

about 3.5% increase in ultimate loads and a 10.6% decrease in the maximum deflection at ultimate loads.

- The crack-propagation patterns confirmed by FEM matched those observed in the experimental investigation rather closely. On the other hand, the specimens failed with a failure mode similar to that recorded in the experimental test.
- When the openings are present, the usual flow of stresses is disrupted or interrupted, which causes stress concentration and early cracking in the area of the opening.
- Increasing openings size increased rate of decrease in the ultimate load.

References

[1] N. K. Raju *Advanced Reinforced Concrete Design*, First Edition ed. CBS Publishers &distributers, 1986.
[2] V. Paramasivam, "Vierendeel Frame Analysis: Slope-Shear Equations," *Journal of the Structural Division*, vol. 106, no. 11, pp. 2333-2339, 1980.
[3] N.A.H.Alwash, "Nonlinear behavior and optimal design of reinforced viereneel trusses," Ph.D. thesis, university of technology, 1995.
[4] I.R.shuber, "Analysis of vierendeel trusses with rigid ended vertical members " M.Sc.thesis, university of technology, 1996.
[5] "Raghda A. Naser "Structural behavior of Slurry Infiltrated Fibrous Reinforced Concrete Vierendeel System"M.S. thesis, Univ. of Babylon, Babil, Iraq, 2023."
[6] S. Bahij, S. K. Adekunle, M. Al- Osta, S. Ahmad, S. U. Al- Dulaijan, and M. K. Rahman, "Numerical investigation of the shear behavior of reinforced ultra- high-performance concrete beams," *Structural Concrete*, vol. 19, no. 1, pp. 305-317, 2018.
[7] Y. Wu, "Shear strengthening of single web prestressed hollow core slabs using externally bonded FRP sheets," 2015.
[8] J. Lubliner, J. Oliver, S. Oller, and E. Oñate, "A plastic-damage model for concrete," *International Journal of solids and structures*, vol. 25, no. 3, pp. 299-326, 1989.
[9] J. R. Homrich and A. E. Naaman, "Stress-strain properties of SIFCON in uniaxial compression and tension," MICHIGAN UNIV ANN ARBOR DEPT OF CIVIL ENGINEERING, 1988.
[10] P. Kmiecik and M. Kamiński, "Modelling of reinforced concrete structures and composite structures with concrete strength degradation taken into consideration," *Archives of civil and mechanical engineering*, vol. 11, no. 3, pp. 623-636, 2011.
[11] R. Malm, "Shear cracks in concrete structures subjected to in-plane stresses," KTH, 2006.
[12] A. Jawdhari and I. Harik, "Finite element analysis of RC beams strengthened in flexure with CFRP rod panels," *Construction and Building Materials*, vol. 163, pp. 751-766, 2018.
[13] I. M. Metwally, "Nonlinear analysis of concrete deep beam reinforced with gfrp bars using finite element method," *Malaysian Journal of Civil Engineering*, vol. 26, no. 2, 2014.

ISSN: 2616 - 9916
www.journalofbabylon.com | Journal.eng@uobabylon.edu.iq | info@journalofbabylon.com

ARTICLE
JOURNAL OF UNIVERSITY OF BABYLON
For ENGINEERING SCIENCES (JUBES)
Vol.31, No.5.| 2023

ISSN: 2616 - 9916
www.journalofbabylon.com | Journal.eng@uobabylon.edu.iq | info@journalofbabylon.com

التحليل اللاخطي للمسنم الفرنديلي المصنوع من الملاط الخرساني المقوى بألياف الحديد

رغدة علي ناصر خالد كريم شدهان

كلية الهندسة/ قسم المدني/ جامعة بابل

raghda.nasser.engh369@student.uobabylon.edu.iq

الخلاصة:

الغرض من هذا البحث هو دراسة التصرف الانشائي للمسنمات الفرنديلية المصنوعة من الملاط الخرساني المقوى بألياف الحديد (السفكون) تحت الحمل المسلط باستخدام التحليل النظري للمسنمات المدروسة. استخدم برنامج الاباكوس لدراسة السلوك اللاخطي لهذه المسنمات بالاعتماد على العناصر المحددة ثلاثية الابعاد. التصرف الانشائي تمثل بالحمل الاقصى نمط التشققات و الهطول. النتائج النظرية تمت مقارنتها مع النتائج العملية التي تم اجراؤها سابقا واظهرت توافق جيد ونمط فشل مشابه للنتائج العملية. وقد وجد بأن وجود الفتحات يتسبب بقطع لمسار الاجهادات مما يتسبب بتركز الاجهادات في منطقة الفتحات والظهور المبكر للتشققات.

الكلمات الدالة: سفكون, اباكوس, المسنم الفرنديلي, الحمل الاقصى, نمط التشققات.